REPORT

PHYSIOLOGY

Fructose-driven glycolysis supports anoxia resistance in the naked mole-rat

Thomas J. Park,[1]*† Jane Reznick,[2]† Bethany L. Peterson,[1] Gregory Blass,[1] Damir Omerbašić,[2] Nigel C. Bennett,[3] P. Henning J. L. Kuich,[4] Christin Zasada,[4] Brigitte M. Browe,[1] Wiebke Hamann,[5] Daniel T. Applegate,[1] Michael H. Radke,[5,6] Tetiana Kosten,[2] Heike Lutermann,[3] Victoria Gavaghan,[1] Ole Eigenbrod,[2] Valérie Bégay,[2] Vince G. Amoroso,[1] Vidya Govind,[1] Richard D. Minshall,[7] Ewan St. J. Smith,[8] John Larson,[9] Michael Gotthardt,[5,6] Stefan Kempa,[4] Gary R. Lewin[2,10]*

The African naked mole-rat's (*Heterocephalus glaber*) social and subterranean lifestyle generates a hypoxic niche. Under experimental conditions, naked mole-rats tolerate hours of extreme hypoxia and survive 18 minutes of total oxygen deprivation (anoxia) without apparent injury. During anoxia, the naked mole-rat switches to anaerobic metabolism fueled by fructose, which is actively accumulated and metabolized to lactate in the brain. Global expression of the GLUT5 fructose transporter and high levels of ketohexokinase were identified as molecular signatures of fructose metabolism. Fructose-driven glycolytic respiration in naked mole-rat tissues avoids feedback inhibition of glycolysis via phosphofructokinase, supporting viability. The metabolic rewiring of glycolysis can circumvent the normally lethal effects of oxygen deprivation, a mechanism that could be harnessed to minimize hypoxic damage in human disease.

In all kingdoms of life, extreme habitats drive adaptive change to enable species to exploit challenging environments. One challenge faced by subterranean mammals that inhabit confined spaces is an atmosphere low in O_2 and high in CO_2. We studied the naked mole-rat's (*Heterocephalus glaber*) adaptation to low-O_2 and high-CO_2 conditions (Fig. 1A), as this eusocial rodent combines a subterranean lifestyle with large colony sizes of up to 280 members (*1*–*3*). CO_2 levels in naked mole-rat burrows can reach 7 to 10%, orders of magnitude higher than in surface air (*4*). Correspondingly, naked mole-rats do not begin to display behavioral avoidance, hyperventilation, or tissue acidosis until CO_2 levels reach 10% (fig. S1, A to E). Even a 5-hour exposure to 80% CO_2 (20% O_2) was not lethal for naked mole-rats (fig. S1F). O_2 levels are low in the burrows of subterranean mammals (as low as 6%) (*5*, *6*), and the mass huddling behavior of naked mole-rats may exacerbate their exposure to hypoxic stress.

To investigate the molecular mechanisms that allow naked mole-rats to overcome hypoxic stress, we subjected them to controlled hypoxia using atmospheric chambers (Fig. 1, B and C), as approved by local ethics committees. Naked mole-rats tolerated a chronic hypoxic environment of 5% O_2 for 5 hours with no apparent ill effects, whereas mice (*Mus musculus*) died in less than 15 min (Fig. 1B). We next exposed animals to 0% O_2 in a chamber flushed with N_2 (10 liters/min). Respiration in mice ceased, on average, 45 ± 5 s after entering the chamber, and none recovered when reexposed to normoxia 20 s later (n = 4 mice) (Fig. 1C). Similarly, naked mole-rats rapidly lost consciousness (in ~30 s) after exposure to 0% O_2, but unlike mice, the naked mole-rats continued to make sporadic breathing attempts for several minutes (mean 250 ± 2.2 s; n = 4 naked mole-rats) (Fig. 1C). After respiration ceased, naked mole-rats were left in 0% O_2 for an additional minute. Surprisingly, all four naked mole-rats started breathing within seconds upon exposure to room air (Fig. 1C), and all rejoined their colony with no sign of neurological or behavioral deficits. In further experiments, naked mole-rats recovered from fixed 10-min (fig. S2, A and B) and 18-min (Fig. 1, D and E) 0% O_2 exposures, but never from a 30-min exposure (Fig. 1F). Respiratory attempts stopped after ~7 min but resumed after 10 min (Fig. 1D). The heart rate dropped within 2 min from a baseline of ~200 beats per minute (bpm) (*7*) to a steady 50 bpm throughout anoxia (Fig. 1E). In mice, the heart rate rapidly and continuously declined until ~6 min, when it was undetectable by electrocardiogram (Fig. 1E). In anoxic conditions, circulating hemoglobin, which shows a high affinity for O_2 (*8*), could provide a minimal O_2 supply to naked mole-rat organs. During anoxia, naked mole-rat body temperature was maintained at 30°C (fig. S3B), the preferred body temperature of these poikilothermic animals (*9*, *10*). However, warming naked mole-rats to 37°C decreased maximum survival times to 6 min, still much longer than mouse survival times (fig. S3C).

Experiments with isolated hearts (Langendorff preparation) exposed to hypoxia (by stopping perfusion with oxygenated buffer for 30 min) showed that left ventricular developed pressure (LVDP) recovered almost completely to pre-ischemic values in naked mole-rats but not in mice (Fig. 1G and table S1). The mouse LVDP never recovered to more than 65% of baseline, even when examined at 30°C. Thus, the ability of the naked mole-rat heart to continue beating under anoxia is supported by an intrinsic cardiac hypoxia resistance. Both hypercapnia and hypoxia lead to pulmonary edema in mice but not in naked mole-rats (fig. S4, A and B).

We postulated that naked mole-rat vital organs survive O_2 deprivation with metabolic suppression similar to hibernation, torpor, or suspended animation–like states (*11*–*13*). Using metabolomics based on gas chromatography–mass spectrometry (GC-MS) (*14*, *15*), we measured quantitative changes in metabolite concentration during anoxia (calibrations in fig. S5) and compared normoxic baseline values to those at 40 s and 10 min (mouse) or 10 and 30 min (naked mole-rat) of anoxia (Fig. 2A). In contrast to mice, only minor changes in the succinate/fumarate ratio (*16*) were observed in naked mole-rat tissues during anoxia, a sign of mitochondrial shutdown (fig. S6). GC-MS metabolomics can resolve hexoses, which allowed us to observe a specific and marked increase in fructose and sucrose concentration in the liver, kidney, and blood of naked mole-rats 10 min into anoxia (Fig. 2, B to D, and fig. S7, A and B). No statistically significant changes in the levels of these sugars were seen in mouse tissues during anoxia (Fig. 2D and fig. S7). The unexpected appearance of high concentrations of fructose (up to 240 μM in blood) and sucrose, a fructose-glucose disaccharide (up to 1.47 mM in blood at 30 min) (fig. S7), in anoxic tissues suggested that these sugars might fuel metabolism under hypoxic conditions. Fructose enters glycolytic metabolism after phosphorylation by ketohexokinase (KHK) and is converted to fructose-1-phosphate (F1P). Fructolysis is prominent in the kidney, which expresses high levels of both the more fructose-selective KHK-C isoform and the less-efficient KHK-A isoform (*17*–*20*). Consistently, we detected

[1]Laboratory of Integrative Neuroscience, Department of Biological Sciences, University of Illinois at Chicago, Chicago, IL 60607, USA. [2]Molecular Physiology of Somatic Sensation, Max Delbrück Center for Molecular Medicine, Berlin, Germany. [3]Department of Zoology and Entomology, University of Pretoria, Pretoria, Republic of South Africa. [4]Integrative Proteomics and Metabolomics, Berlin Institute for Medical Systems Biology, Max Delbrück Center for Molecular Medicine, Berlin, Germany. [5]Neuromuscular and Cardiovascular Cell Biology, Max Delbrück Center for Molecular Medicine, Berlin, Germany. [6]German Centre for Cardiovascular Research (DZHK), Berlin, Germany. [7]Departments of Anesthesiology and Pharmacology, University of Illinois at Chicago, Chicago, IL 60612, USA. [8]Department of Pharmacology, University of Cambridge, Cambridge CB2 1PD, UK. [9]Department of Psychiatry, University of Illinois at Chicago, Chicago, IL 60612, USA. [10]Excellence Cluster Neurocure, Charité Universitätsmedizin Berlin, Berlin, Germany.
***Corresponding author. Email: glewin@mdc-berlin.de (G.R.L.); tpark@uic.edu (T.J.P.)** †These authors contributed equally to this work.

high levels of F1P in the kidney, which were unaltered after anoxia in both species (Fig. 2D). However, F1P was undetectable in normoxic brains but appeared in significant amounts only in anoxic naked mole-rat brains, indicating a switch to fructose metabolism (Fig. 2D). Surprisingly, naked mole-rats were hypoglycemic compared with mice (mean blood glucose 3.49 ± 0.1 versus 6.66 ± 0.3 mM in mice) (fig. S8A) (*21*), but during anoxia, naked mole-rat glucose levels did not show consistent changes divergent from those in the mouse (fig. S8). Furthermore, although there were some differences in glycogen stores between the two species, these were relatively small and not consistent across all tissues (fig. S8).

Fructose can enter cells via GLUT2 and GLUT5, which belong to the SLC2A transporter family (*17*, *22*). The GLUT5 (SLC2A5) protein is a highly selective fructose transporter (*18*) predominantly expressed in the mouse intestine and kidney but hardly present in the brain and heart (*17*). Using quantitative real-time polymerase chain reaction (qPCR), we found that naked mole-rat *GLUT5* mRNA (Slc2a5) (fig. S9A) was expressed at high levels (>10-fold higher than mouse) in all examined tissues, including the brain, heart, liver, and lung (Fig. 2E). As analyzed with Western blotting, GLUT5 protein levels were higher in naked mole-rat heart and brain tissue compared with mouse, and levels broadly reflected mRNA levels (Fig. 2F and fig. S9C). Thus, naked mole-rat brain and cardiac tissue likely take up fructose for glycolytic metabolism. Consistently, both KHK isoforms were markedly up-regulated in naked mole-rat heart, brain, and liver tissue compared with the same tissues in mice (Fig. 2G and fig. S9B).

Brain tissue from naked mole-rats shows a pronounced, intrinsic tolerance to anoxia (*19*). We thus tested whether naked mole-rat brains can function by using fructose-fueled glycolytic metabolism. We measured field excitatory postsynaptic potentials (fEPSPs) in hippocampal slices from mouse and naked mole-rat hippocampi (n = 3 animals per species) before and 60 min after replacement of 10 mM glucose in the buffer with 10 mM fructose (normoxic conditions). With fructose as the sole available sugar, fEPSP amplitude declined steadily but at different rates in mouse and naked mole-rat slices (Fig. 3A). In mice, fEPSPs were almost undetectable 60 min after the glucose-to-fructose switch, but fEPSP amplitudes in naked mole-rat slices had stabilized to ~33% of control values. After slices were reperfused with glucose-containing buffer, mean fEPSP amplitudes returned to control levels in naked mole-rat slices but only partially recovered in mouse slices [two-way analysis of variance (ANOVA), $P < 0.05$] (Fig. 3A). We also examined whether fructose could be used to fuel the isolated beating heart. Naked mole-rat or mouse hearts were perfused with Krebs-Henseleit buffer containing glucose that was then switched to fructose for two periods of 60 min each. The LVDP of the naked mole-rat hearts remained stable during both fructose switches. However, in the mouse heart, LVDP was reduced during both fructose exposures and differed significantly from that of naked mole-rat hearts during the latter exposure (Fig. 3B). Thus, fructose can replace glucose as an energy source in the naked mole-rat brain and heart.

Glucose is metabolized via phosphofructokinase (PFK), a rate-limiting step subject to feedback inhibition via allosteric binding of adenosine triphosphate, low pH, and downstream intermediates (*8*, *20*, *23*) (Fig. 4A). Fructose phosphorylation via KHK could bypass the PFK regulatory block, allowing continued glycolytic flux independent of cellular energy status. We used metabolic flux analysis to measure the incorporation of fructose-derived carbons into glycolytic intermediates in hypoxic brain slices. Acutely isolated brain slices were incubated in media in which glucose was rapidly replaced with the stable isotope $^{13}C_6$-D-fructose (10 mM) and were kept at 32°C with 5% O_2 levels (*24*). Metabolites were measured at 0, 5, 15, and 30 min after the switch to $^{13}C_6$-D-fructose. Similar metabolite pools were detected in both species, suggesting that metabolism was at the same steady state in both species (fig. S10). We could measure significant incorporation of fructose-derived carbons in glycolytic intermediates in both species (Fig. 4, A to H), but

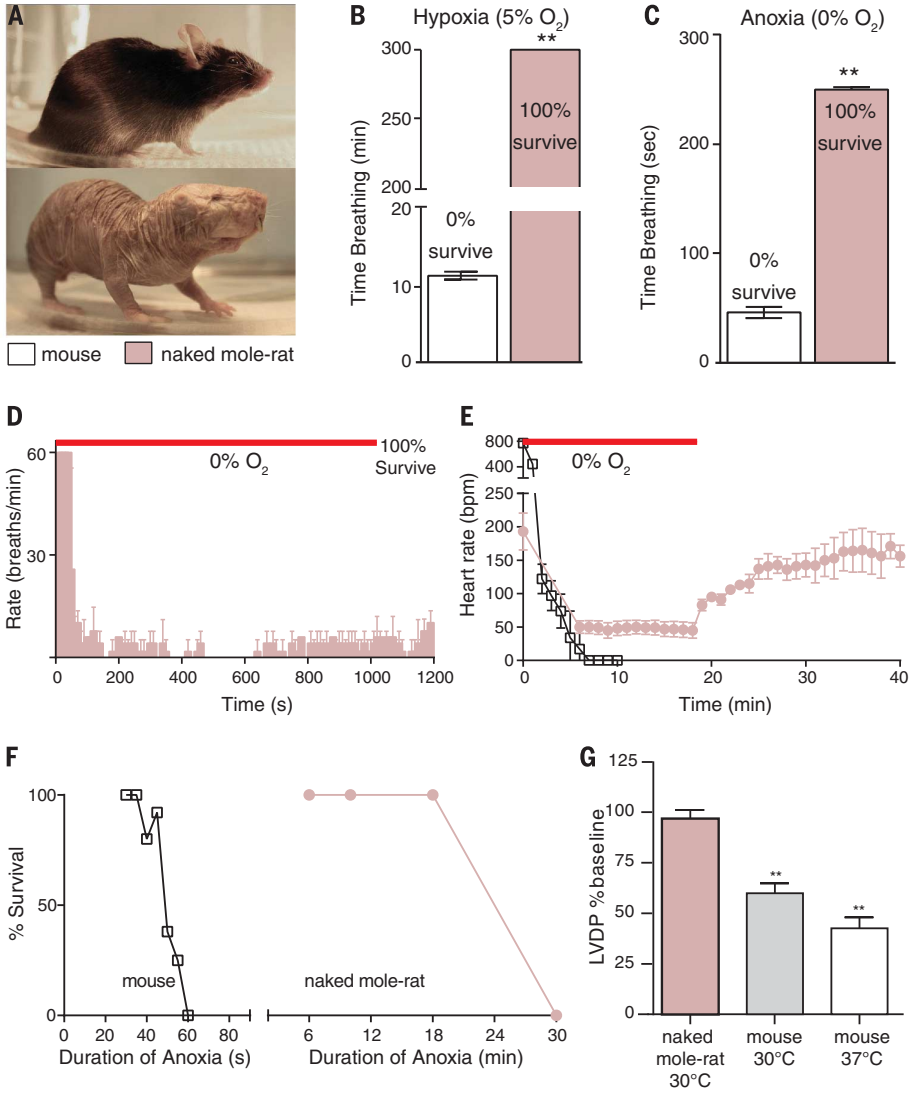

Fig. 1. Extreme hypoxia and anoxia resistance in naked mole-rats. (**A**) Mouse (top) and naked mole-rat (bottom). (**B** and **C**) Time breathing in 5% O_2 (cut-off time: 300 min) (B) or in anoxia (0% O_2, cut-off: last breath) (C). Naked mole-rats always survived; mice did not (n = 4 to 6 animals per group, $^{**}P < 0.01$; Fisher's exact test). Survival rate after exposure to 0% O_2 was significantly different between species ($^{**}P < 0.001$; Student's t test). (**D**) Respiration and (**E**) heart rate during 18 min of 0% O_2 (n = 4 animals per species). (**F**) Survival plotted against duration of complete anoxia for mice and naked mole-rats (n = 3 to 12 animals per species and time point). (**G**) Left ventricular developed pressure (LVDP) measured in isolated hearts after a 30-min period of hypoxia induced by stopping the coronary flow. Results were compared with baseline values ($^{**}P < 0.01$; two-way ANOVA with Bonferroni post hoc test; n = 3 animals per group). Mean ± SEM (error bars).

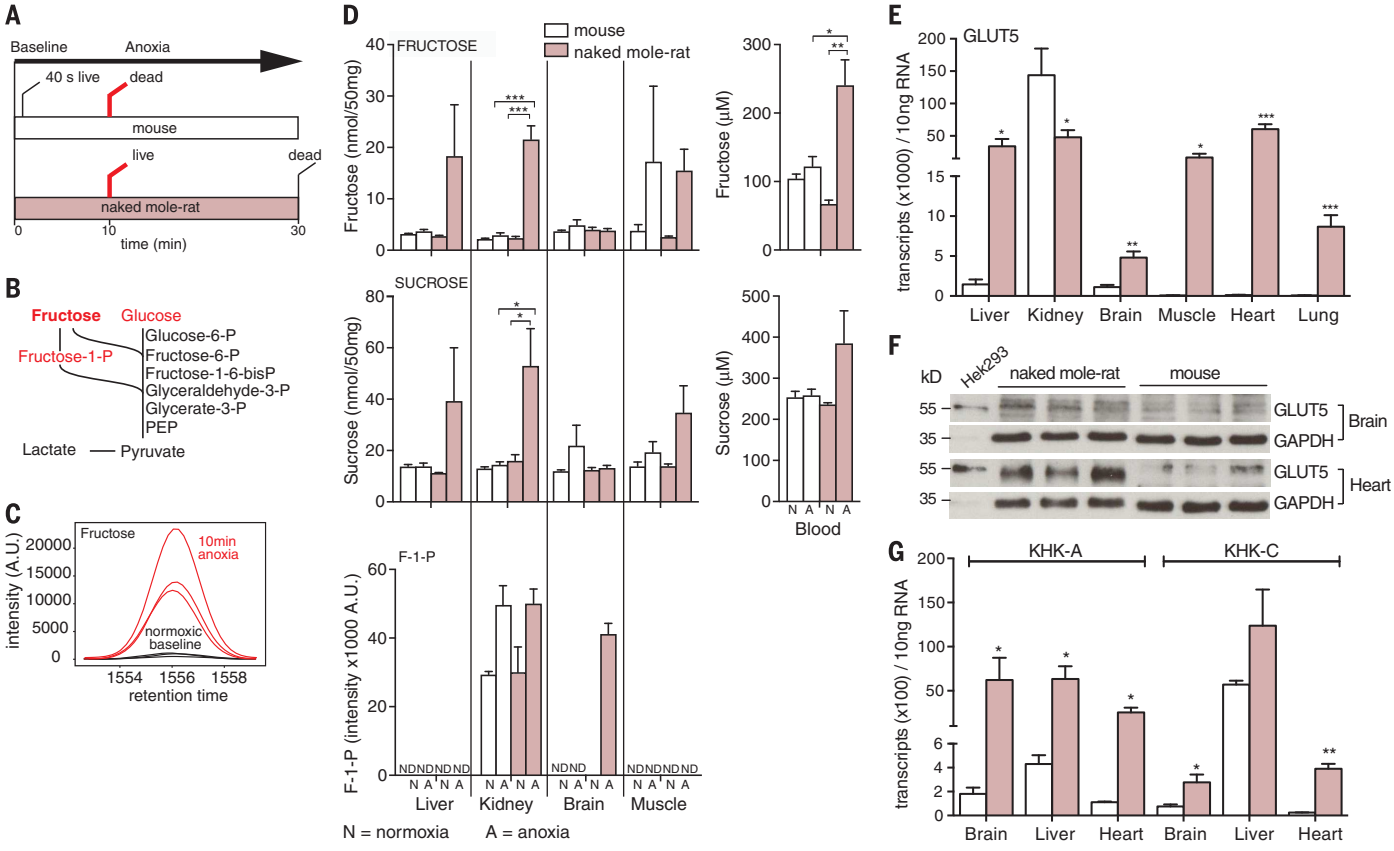

Fig. 2. Fructose and sucrose in anoxia-exposed naked mole-rats. (**A**) Experimental design. (**B** and **C**) Metabolic intermediates were quantified using GC-MS. P, phosphate; PEP, phosphoenolpyruvate. (C) Increased fructose in anoxia-exposed naked mole-rat kidneys (chromatograms of species triplicates). A.U., arbitrary units. (**D**) Quantification of fructose, sucrose, and fructose-1-phosphate (F-1-P) levels (concentrations or peak intensity) before and after anoxia. N, normoxia; A, anoxia; ND, not detected (n = 3 animals per species; error bars indicate SEM; $^{*}P < 0.05$; $^{**}P < 0.01$, $^{***}P < 0.001$ using a two-way ANOVA with Bonferroni's post hoc test). (**E**) Expression level of GLUT5 mRNA transcripts in mouse and naked mole-rat tissues evaluated by qPCR (n = 3 animals per species; error bars indicate SEM; $^{*}P < 0.05$; $^{***}P < 0.001$; two-tailed unpaired t test). (**F**) Western blot for GLUT5 in brain and heart tissues from both species (three biological replicates). GAPDH, glyceraldehyde-3-phosphate dehydrogenase. (**G**) Bar graphs showing results of qPCR designed to detect KHK-C and KHK-A isoforms (n = 3 animals per species; error bars indicate SEM; $^{*}P < 0.05$; $^{**}P < 0.01$; two-tailed unpaired t test).

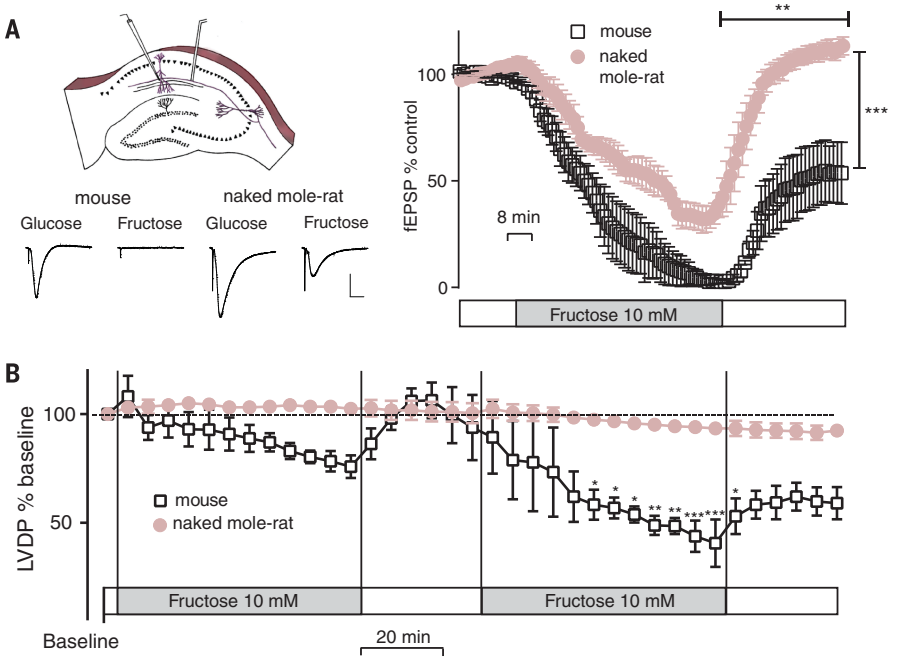

Fig. 3. Role of fructose in maintaining brain and heart function in naked mole-rats. (**A**) Field excitatory postsynaptic potentials (fEPSPs) were recorded in hippocampal brain slices. fEPSP amplitude declined to zero when fructose replaced glucose in mouse slices but was maintained in naked mole-rat slices. Example traces are shown at left below the diagram [scale bar, 1 mV (vertical) and 10 msec (horizontal)]. A two-way repeated measures ANOVA with Bonferroni post hoc test ($^{**}P < 0.01$) revealed significant effects for species ($F_{1,4}$ = 19.8, P = 0.0114) and time ($F_{99,396}$ = 43.43, $^{***}P < 0.0001$). The interaction between group and time was also significant ($F_{99,396}$ = 6.16, $^{***}P < 0.0001$). n = 3 animals per species; error bars indicate SEM. (**B**) LVDP was measured for isolated hearts after glucose replacement with fructose. Naked mole-rat LVDP was maintained but mouse LVDP declined, especially after a second exposure to fructose. Statistical significance was calculated with a two-way ANOVA. Error bars indicate SEM.

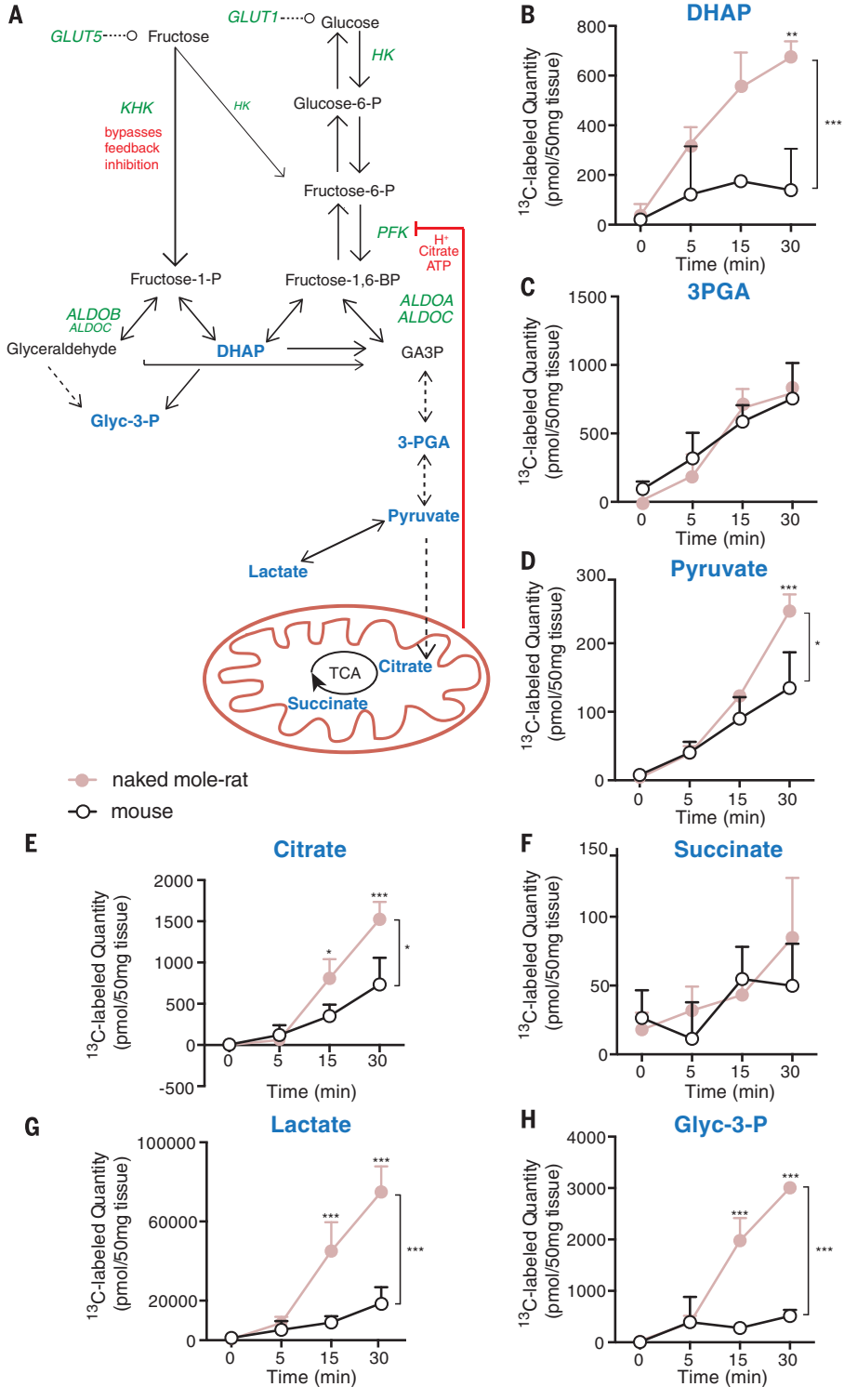

Fig. 4. Metabolic flux of fructose metabolites in the hypoxic brain. (**A**) Glycolysis pathway. Glucose enters the brain via GLUT1 and is converted via phosphofructokinase (PFK). Fructose enters cells via GLUT5 and is phosphorylated by ketohexokinase (KHK) to fructose-1-phosphate (F1P) at a much higher efficiency than by hexokinase (HK). F1P is directly metabolized into trioses via aldolase B (ALDOB) or aldolase C (ALDOC), bypassing feedback inhibition. GA3P, glyceraldehyde-3-phosphate; TCA, tricarboxylic acid. (**B** to **H**) Incorporation of ^{13}C-fructose–derived carbons was measured during acute hypoxia (~5% O_2) at 0, 5, 15, and 30 min. Labeled quantities of the different metabolic intermediates (in blue) are shown. (B) Dihydroxyacetone phosphate (DHAP). (C) Phosphoglyceric acid (3PGA). (D) Pyruvate. (E) Citrate. (F) Succinate. (G) Lactate. (H) Glycerol-3-phosphate (Glyc-3-P). $n = 3$ animals per species; error bars indicate SEM; $^{*}P < 0.05$; $^{**}P < 0.01$, $^{***}P < 0.001$ using a two-way ANOVA with a Bonferroni's post hoc test.

the incorporation of fructose-derived carbons was both faster and larger in the naked mole-rat compared with the mouse (between two- and fivefold). This observation was found to be true for intermediates such as dihydroxyacetone phosphate (DHAP) and glycerol-3-phosphate (Glyc-3-P) (Fig. 4, B and H) but also for glycolytic end products like pyruvate and lactate (Fig. 4, D and G). Increased fructose-derived carbon incorporation into citrate was also observed in the naked mole-rat (Fig. 4E).

The naked mole-rat has evolved the ability to use fructose to fuel vital organs such as the heart and brain under near-anaerobic conditions. This metabolic rewiring involves equipping metabolically active organs with transporters and enzymes that metabolize fructose to lactate using a pathway that bypasses metabolic block at PFK (Fig. 4A). Fructose and sucrose (the latter is degraded to hexose monomers) are both increased to statistically significant levels in the naked mole-rat during anoxia. The source of these sugars is unknown. Fructolysis in mammals is normally largely restricted to the liver and kidney (*25*). A switch to fructose metabolism under hypoxic stress has been associated with cancer malignancy, metabolic syndrome, and heart failure (*26*–*29*). It is thus important to understand how naked mole-rats utilize fructose metabolism with no apparent physiological drawbacks. Molecular insights into the rewired metabolism of the naked mole-rat may help in devising strategies to prevent hypoxic damage associated with ischemic heart disease and stroke.

REFERENCES AND NOTES

1. J. U. Jarvis, *Science* **212**, 571–573 (1981).
2. P. W. Sherman, J. U. M. Jarvis, R. D. Alexander, Eds., *The Biology of the Naked Mole-Rat* (Monographs in Behavior and Ecology, Princeton Univ. Press, 1991).
3. L.-N. Schuhmacher, Z. Husson, E. S. Smith, *Open Access Anim. Physiol.* **7**, 137–148 (2015).
4. B. K. McNab, *Ecology* **47**, 712–733 (1966).
5. I. Shams, A. Avivi, E. Nevo, *Comp. Biochem. Physiol. A* **142**, 376–382 (2005).
6. H. Burda, R. Šumbera, S. Begall, in *Subterranean Rodents: News From Underground*, S. Begall, H. Burda, C. E. Schleich, Eds. (Springer, 2007), pp. 21–33.
7. K. M. Grimes, A. K. Reddy, M. L. Lindsey, R. Buffenstein, *Am. J. Physiol. Heart Circ. Physiol.* **307**, H284–H291 (2014).
8. S. Lenzen, *J. Biol. Chem.* **289**, 12189–12194 (2014).
9. N. C. Bennett, C. G. Faulkes, *African Mole-Rats: Ecology and Eusociality* (Cambridge Univ. Press, 2000).
10. R. Buffenstein, S. Yahav, *J. Therm. Biol.* **16**, 227–232 (1991).
11. E. Blackstone, M. Morrison, M. B. Roth, *Science* **308**, 518 (2005).
12. J. F. Staples, J. C. L. Brown, *J. Comp. Physiol. B* **178**, 811–827 (2008).
13. K. B. Storey, *Gerontology* **56**, 220–230 (2010).
14. M. Pietzke, C. Zasada, S. Mudrich, S. Kempa, *Cancer Metab.* **2**, 9 (2014).
15. P. H. J. L. Kuich, N. Hoffmann, S. Kempa, *Front. Bioeng. Biotechnol.* **2**, 84 (2015).
16. R. Narsai, M. Rocha, P. Geigenberger, J. Whelan, J. T. van Dongen, *New Phytol.* **190**, 472–487 (2011).
17. V. Douard, R. P. Ferraris, *Am. J. Physiol. Endocrinol. Metab.* **295**, E227–E237 (2008).
18. C. F. Burant, J. Takeda, E. Brot-Laroche, G. I. Bell, N. O. Davidson, *J. Biol. Chem.* **267**, 14523–14526 (1992).
19. J. Larson, T. J. T. Park, *Neuroreport* **20**, 1634–1637 (2009).
20. P. B. Garland, P. J. Randle, E. A. Newsholme, *Nature* **200**, 169–170 (1963).
21. R. Buffenstein, M. Pinto, *Mol. Cell. Endocrinol.* **299**, 101–111 (2009).

22. A. R. Manolescu, K. Witkowska, A. Kinnaird, T. Cessford, C. Cheeseman, *Physiology* **22**, 234–240 (2007).
23. G. P. Dobson, E. Yamamoto, P. W. Hochachka, *Am. J. Physiol. Regul. Integr. Comp. Physiol.* **250**, R71–R76 (1986).
24. G. Mauleon, J. F. Lo, B. L. Peterson, C. P. Fall, D. T. Eddington, *J. Neurosci. Methods* **216**, 110–117 (2013).
25. J. Hallfrisch, *FASEB J.* **4**, 2652–2660 (1990).
26. A. M. Port, M. R. Ruth, N. W. Istfan, *Curr. Opin. Endocrinol. Diabetes Obes.* **19**, 367–374 (2012).
27. H. Liu *et al.*, *Cancer Res.* **70**, 6368–6376 (2010).
28. L. Tappy, K.-A. Lê, *Physiol. Rev.* **90**, 23–46 (2010).
29. P. Mirtschink *et al.*, *Nature* **522**, 444–449 (2015).

ACKNOWLEDGMENTS

This work was supported the European Research Council (grant 294678), the Deutsche Forschungsgemeinschaft (grants SFB 665 and Go865/9-1), the NSF (grant 0744979), and the NIH (grants HL71626 and HL60678). Technical support was provided by M. Braunschweig, F. Kressin, M. Pippow, and D. J. Visintine. All relevant data are stored at the Max Delbrück Center for Molecular Medicine and are available from the authors upon request or are included in the manuscript and supplementary materials. The project was conceived and coordinated by G.R.L., T.J.P., J.R., M.G., S.K., and N.C.B. Experiments were performed by J.R., B.L.P., G.B., D.O., W.H., M.H.R., V.B., R.D.M., B.M.B., J.L., D.T.A., E.St.J.S., V.Ga., V.Go., V.G.A., H.L., N.C.B., T.J.P., G.R.L., R.D.M., and E.St.J.S. Data analysis and bioinformatics were carried out by J.R., P.H.J.L.K., C.Z., O.E., T.K., S.K., W.H., M.H.R., and M.G. The paper was written by G.R.L., T.J.P., and J.R. with input from all authors. Contact S.K. for correspondence on metabolomics.

SUPPLEMENTARY MATERIALS

www.sciencemag.org/content/356/6335/307/suppl/DC1
Materials and Methods
Figs. S1 to S10
Table S1
References (*30*–*33*)
Data S1

13 June 2016; accepted 1 March 2017
10.1126/science.aab3896

Fructose-driven glycolysis supports anoxia resistance in the naked mole-rat

Thomas J. Park, Jane Reznick, Bethany L. Peterson, Gregory Blass, Damir Omerbasic, Nigel C. Bennett, P. Henning J. L. Kuich, Christin Zasada, Brigitte M. Browe, Wiebke Hamann, Daniel T. Applegate, Michael H. Radke, Tetiana Kosten, Heike Lutermann, Victoria Gavaghan, Ole Eigenbrod, Valérie Bégay, Vince G. Amoroso, Vidya Govind, Richard D. Minshall, Ewan St. J. Smith, John Larson, Michael Gotthardt, Stefan Kempa and Gary R. Lewin

Science **356** (6335), 307-311.
DOI: 10.1126/science.aab3896

Safe anaerobic metabolism

Naked mole-rats live in large colonies deep underground in hypoxic conditions. Park *et al.* found that these animals fuel anaerobic glycolysis with fructose by a rewired pathway that avoids tissue damage (see the Perspective by Storz and McClelland). These results provide insight into the adaptations that this strange social rodent has to make for life underground. They also have implications for medical practice, particularly for understanding how to protect tissues from hypoxia.

Science, this issue p. 307; see also p. 248